BULLETIN OF THE POLISH ACADEMY OF SCIENCES
TECHNICAL SCIENCES, Vol. 73(3), 2025, Article number: e154272
DOI: 10.24425/bpasts.2025.154272

Discrete non-integer order model of synchronous generator for power hardware-in-the-loop implementation

Szymon RACEWICZ[1]*, **Filip KUTT**[2], **Łukasz SIENKIEWICZ**[2], **Michał MICHNA**[2], and **Roland RYNDZIONEK**[2]

[1] University of Warmia and Mazury in Olsztyn, Faculty of Technical Sciences, ul. Oczapowskiego 11, 10-719 Olsztyn, Poland
[2] Gdańsk University of Technology, Faculty of Electrical and Control Engineering, ul. Gabriela Narutowicza 11/12, 80-233 Gdańsk, Poland

Abstract. Non-integer order modelling is used for a better description of different natural physical phenomena, which leads to more compact and knowledge-based models. The main objective of the presented study is to apply the non-integer order model of a synchronous generator (SG) in the power hardware-in-the-loop (PHIL) technique, which is readily used for design, research and development, maintenance, or service purposes. The developed model was prepared and run in the MATLAB/Simulink software using a discrete solver. To discretize the non-integer order model, the Z-transform was applied and the half-order derivatives and integrals present in the model equations were evaluated using Oustaloup approximation. Finally, the model was validated on the measurements of the 125 kVA SG connected to the active-reactive loads of different values and compared with the classical integer order one.

Keywords: non-integer order modelling; synchronous generator; power hardware-in-the-loop; PHIL.

1. INTRODUCTION

The non-integer order modelling is well known as a powerful approach used for precise and pertinent modelling of different natural phenomena like diffusion (of electric fields, temperature, gases, liquids) [1, 2], energy and heat transfer [3, 4], proton exchange [5], electrochemical reactions [6], skin effect [7], eddy currents [8, 9], etc. Non-integer order modelling has been increasingly adopted in recent years for the development of behavioural models of devices such as car suspensions [10], batteries [11], super and ultracapacitors [12, 13], fuel cells [14] or electrical machines [15–17]. It is also used for robust controller design [18]. Non-integer order modelling offers enhanced modelling capabilities for various complex systems as it extends traditional integer-order calculus to non-integer order derivatives and integrals providing more flexible tools for describing system dynamics. Non-integer order models naturally incorporate memory, meaning that the current state depends not only on the present but also on the history of the system. It further implies spatial and temporal non-locality, which means that models account for interactions over a range of space and time, rather than just local interactions. Additionally, the non-integer order models provide better flexibility in data fitting due to their additional degrees of freedom. All these features reduce the parameter number in the non-integer order models, as compared to the integer-order ones and, at the same time enhance their accuracy, especially in frequency domain analysis [19]. Indeed, this last characteristic is regarded as a kind of inconvenience as for the time domain analysis in industry applications (e.g., PHIL platforms), the fractional order transmittances need to be approximated by integer order ones [20]. In this context, it is interesting to verify further the usefulness of the non-integer order modelling approach in time-related applications, e.g., the power hardware-in-the-loop technique (PHIL).

The PHIL approach has been gaining in popularity in recent years. It consists of running the simulation model on the hardware platform with an I/O interface enabling the real signals to be analyzed and tested. Such an approach allows for designing a scalable so-called "digital twin" [21] or emulator of a studied machine without the need to construct an expensive and space-consuming full-scale system [22]. Several industrial branches, especially the aviation industry [23] or marine industry [24, 25] have adopted this solution for efficient testing and prototyping the new ideas in distribution power systems comporting more and more electrical components, e.g., battery energy storage systems (BESS), fuel cells, power management systems (PMS) or solar and wind renewable energy sources. These increasingly complex structures of today's modern distributed smart grid power systems require the application of tools allowing for flexible analysis of the behaviour, reliability, or readiness of system components.

In the latest literature, one can find some useful hardware-in-the-loop (HIL) and PHIL solutions dedicated to reliability, maintenance, or service purposes that can be safely implemented in laboratory conditions. In [26], the authors proposed the PHIL solution that incorporates an AC/DC converter model for the

*e-mail: szymon.racewicz@uwm.edu.pl

Manuscript submitted 2024-09-02, revised 2025-02-12, initially accepted for publication 2025-03-25, published in May 2025.

simulation of a 20-kW DC nano grid to study the stability and reliability of the grid under fault conditions, i.e., blackouts and short circuits. The results proved that the developed testbed is appropriate for studying the nano DC grid performance which allows for avoiding inconvenient and dangerous tests on real power systems. In [27], the PHIL solution of wave energy converter (WEC) serves to adapt the Bayesian policy gradient-based WEC control approach, which is adaptive to faults in controller feedback, actuation, and plant model changes. In this case, the PHIL solution contributes to mitigating the costs of operation, maintenance, and repair as the wave energy converters are usually off-shore technologies. The paper [28] describes the hardware-in-the-loop (HIL) tests based on the RT-LAB simulation platform. They were performed to illustrate the performance of the ageing rate equalization strategy for microgrid-scale BESSs. Finally, the article [29] focuses on the PHIL emulator of induction motors with internal faults. The proposed solution uses a mathematical model of a faulted induction machine, which reduces the costs, risk, and time associated with the real faults generation need [30–32]. Also, the accuracy and reliability of PHIL platforms themselves have been widely discussed in the recent literature [33–35] to ensure the effective usability of such solutions.

The above-mentioned research shows a vital interest in PHIL system development. Albeit, the presented PHIL solutions are mostly based on classical integer order equations. In this article, we use the non-integer order differential equations to formulate the SG model for PHIL application based on the bidirectional DC/AC power converter.

The main highlights of the article are as follows:

- Development of discrete non-integer order model of synchronous generator.
- Implementation of power hardware-in-the-loop technique based on commercial-grade power converter.
- Comparison with integer order model of synchronous generator.
- MATLAB/Simulink simulations of transient states of the power generation unit.

2. NON-INTEGER ORDER MODEL OF SG

Figure 1 shows the SG non-integer order equivalent circuits (axes d and q) with half-order impedances $Z_{1d}^{1/2}$, $Z_{1q}^{1/2}$, $Z_{2d}^{1/2}$ integrated into the model.

This model was extensively discussed in the previous authors' papers [19, 36–38] in terms of accuracy, parameter identification procedure, and time-domain simulations. The key feature distinguishing the presented model from other approaches is its ability to operate accurately in higher frequency ranges by modelling also effects such as skin and eddy currents developing during transient states without increasing the overall order of the model. Indeed, starting with the Maxwell equations, the structure as well as the circuit parameters were derived. The $Z_{1d}^{1/2}$ and $Z_{1q}^{1/2}$ half-order inductive impedances are used to model massive ferromagnetic parts of the machine rotor in d and q axes and are given by equation (1) in *explicit* form, whereas $Z_{2d}^{1/2}$ half-order resistive impedance is used to model squirrel cage damper bars

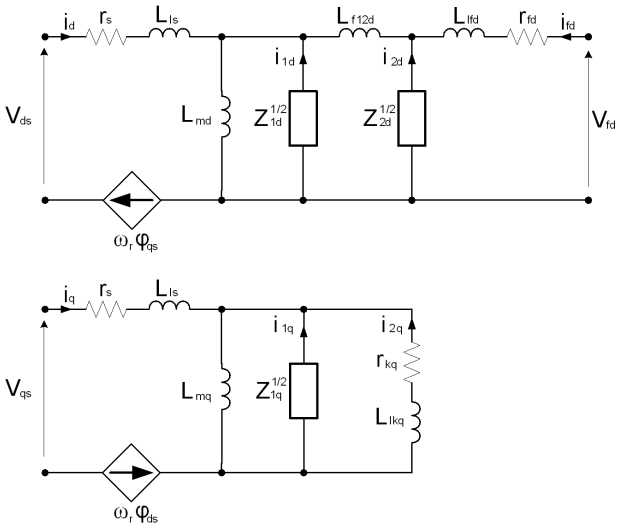

Fig. 1. Non-integer order equivalent circuits of SG (axes d and q)

in the d-axis and is given by equation (2) in *explicit* form. In all equations, s denotes the Laplace operator equal to $j \cdot 2\pi f$

$$Z_{1d/1q}^{1/2}(s) = \frac{L_{1d/1q} \cdot s}{1 + \sqrt{\dfrac{s}{\omega_{1d/1q}}}}, \tag{1}$$

$$Z_{2d}^{1/2}(s) = R_{2d} \cdot \left(1 + \sqrt{\frac{s}{\omega_{2d}}}\right). \tag{2}$$

Coefficients $L_{1d/1q}$ and R_{2d} of the above non-integer order impedances are called DC inductance and DC resistance respectively and can be identified from the SSFR test procedure or, for the simple geometry elements, calculated directly from the physical properties and dimensions of the modelled parts [36]. Similarly, for the $\omega_{1d/1q}$ and ω_{2d} which are the cut-off frequencies of the half-order systems.

Finally, the system of equations defining the non-integer order SG model in the orthogonal d-q reference frame is given in (3)

$$\begin{cases} V_{ds} = r_s \cdot i_{ds} - \omega_r \varphi_{qs} + s \cdot \varphi_{ds}, \\ V_{qs} = r_s \cdot i_{qs} + \omega_r \varphi_{ds} + s \cdot \varphi_{qs}, \\ 0 = Z_{1d}^{1/2} \cdot i_{1d} + s \cdot \varphi_{1d}, \\ 0 = Z_{2d}^{1/2} \cdot i_{2d} + s \cdot \varphi_{2d}, \\ 0 = Z_{1q}^{1/2} \cdot i_{1q} + s \cdot \varphi_{1q}, \\ 0 = r_{kq} \cdot i_{2q} + s \cdot \varphi_{2q} + s \cdot \varphi_{1q}, \\ V_{fd} = r_{fd} \cdot i_{fd} + s \cdot \varphi_{fd}. \end{cases} \tag{3}$$

With the flux components defined as (4), (5), (6), (7), (8), (9) and (10)

$$\varphi_{ds} = L_{ls} \cdot i_{ds} + L_{md}\left(i_{ds} + i_{1d} + i_{2d} + i_{fd}\right), \tag{4}$$

$$\varphi_{qs} = L_{ls} \cdot i_{qs} + L_{mq}\left(i_{qs} + i_{1q} + i_{2q}\right), \tag{5}$$

$$\varphi_{1d} = L_{md}\left(i_{ds} + i_{1d} + i_{2d} + i_{fd}\right), \tag{6}$$

$$\varphi_{1q} = L_{mq}\left(i_{qs} + i_{1q} + i_{2q}\right), \tag{7}$$

$$\varphi_{2d} = L_{md}\left(i_{ds}+i_{1d}+i_{2d}+i_{fd}\right)+L_{f12d}\left(i_{2d}+i_{fd}\right), \tag{8}$$

$$\varphi_{2q} = L_{lkq}\cdot i_{2q}, \tag{9}$$

$$\varphi_{fd} = L_{lfd}\cdot i_{fd}+L_{f12d}\left(i_{2d}+i_{fd}\right) + L_{md}\left(i_{ds}+i_{1d}+i_{2d}+i_{fd}\right), \tag{10}$$

where V_{ds} and V_{qs} are the armature voltages in the d-q reference frame; V_{fd} is the excitation voltage; i_{ds} and i_{qs} are the armature currents in the d-q reference frame; i_{fd} is the excitation current; i_{1d} and i_{1q} are the currents modelling the effects of eddy currents present in the solid steel elements of the rotor in the d and q axes; i_{2d} and i_{2q} are the currents modelling the skin effects in damper windings in the d and q axes, taking into account the fact that for identification reasons the damper bars in the q-axis are modelled by the classical resistance r_{kq} and the classical inductance L_{lkq} both constant with frequency. Next, φ_{ds} and φ_{qs} are the armature flux linkages in the d-q reference frame; φ_{1d}, φ_{2d}, φ_{1q} and φ_{2q} are the appropriate massive parts and damper windings flux linkages in the d-q reference frame; φ_{fd} is the excitation flux linkage and ω_r is the electrical angular speed of the machine. L_{md} and L_{mq} are the magnetizing mutual inductances of the machine in the d-q reference frame; L_{ls} and L_{lfd} are the leakage inductance of armature windings and the leakage inductance of field winding respectively; L_{f12d} is the mutual inductance linking field and damper windings. The rated data of the studied SG and the identified model parameters can be found in the Appendix. The parameter identification process was performed based on data from the standstill frequency response test (SSFR) and the least-squares method algorithm [39].

Equations (11) and (12) describe the mechanical comportment of the dynamometer driving machine and the SG unit. T_l is the driving torque set by the proportional-integral regulator (PI); T_e is the electromagnetic torque of the machine; B_m is the mechanical loss coefficient; J is the inertia coefficient of the unit shaft and p stands for the pole pair number.

$$s\cdot\omega_r = \frac{p}{J}\left(T_l - T_e - B_m\omega_r\right), \tag{11}$$

$$T_e = \frac{3p}{2}\left(\varphi_{ds}i_{qs}-\varphi_{qs}i_{ds}\right). \tag{12}$$

Integrating the equations (1) and (2) into the system equation (3) one obtains the following system equations (13) with the Laplace operator s to the powers of 1 and 1/2 which represents the non-integer order derivatives

$$\begin{cases} V_{ds} = r_s\cdot i_{ds}-\omega_r\varphi_{qs}+s\cdot\varphi_{ds}, \\ V_{qs} = r_s\cdot i_{qs}+\omega_r\varphi_{ds}+s\cdot\varphi_{qs}, \\ 0 = L_{1d}\cdot i_{1d}+\varphi_{1d}+\dfrac{1}{\sqrt{\omega}_{1d}}\cdot s^{1/2}\cdot\varphi_{1d}, \\ 0 = R_{2d}\cdot i_{2d}+s\cdot\varphi_{2d}+\dfrac{R_{2d}}{\sqrt{\omega}_{2d}}\cdot s^{1/2}\cdot i_{2d}, \\ 0 = L_{1q}\cdot i_{1q}+\varphi_{1q}+\dfrac{1}{\sqrt{\omega}_{1q}}\cdot s^{1/2}\cdot\varphi_{1q}, \\ 0 = r_{kq}\cdot i_{2q}+s\cdot\varphi_{2q}+s\cdot\varphi_{1q}, \\ V_{fd} = r_{fd}\cdot i_{fd}+s\cdot\varphi_{fd}. \end{cases} \tag{13}$$

3. NON-INTEGER ORDER MODEL IMPLEMENTATION

PHIL platforms based on real-time simulations require discretization of the model equations. The authors proposed a PHIL platform based on the bidirectional DC/AC commercial-grade power converter. Such a system requires compiling the Simulink model into the C code which is then loaded to the power converter real-time controller. For this purpose, the equation system (13) needs to be implemented in the MATLAB/Simulink software using discrete form and the Z-transform. Even though MATLAB has many toolboxes and libraries, there is no solution to model a fractional order differential equation using the Z-transform of the non-integer order. To tackle this issue, it is unavoidable to use an approximation of the fractional order systems by integer order ones. One of the most useful and pertinent methods dedicated to such an approximation in the frequency domain $[\omega_b, \omega_h]$ is the Oustaloup method [40]. The basic equations of the Oustaloup filter for $G(s) = s^{\alpha}$ where α is a non-integer number and N is an approximation order are given below by (14), (15), (16), (17) and (18) [41]

$$G(s) = K\prod_{i=-N}^{N}\frac{s+\omega_i'}{s+\omega_i}, \tag{14}$$

where

$$K = \sqrt{\frac{\omega_b}{\omega_h}}^{\alpha}, \tag{15}$$

$$\omega_i' = \omega_b\left(\frac{\omega_h}{\omega_b}\right)^{\frac{i+N+\frac{1}{2}-\frac{n}{2}}{2N+1}}, \tag{16}$$

$$\omega_i = \omega_b\left(\frac{\omega_h}{\omega_b}\right)^{\frac{i+N+\frac{1}{2}+\frac{n}{2}}{2N+1}}, \tag{17}$$

$$N = \frac{\log\left(\dfrac{\omega_N}{\omega_0}\right)}{\log\left(\dfrac{\omega_{i+1}}{\omega_i}\right)}. \tag{18}$$

In the MATLAB/Simulink software, the Oustaloup approximation is present among others in the "fractional-order modelling and control" toolbox (FOMCON) developed by Tepljakov, Petlenkov, and Belikov in 2011 [42]. Exemplary blocks from this toolbox are: "discrete transfer Fcn", "fractional state-space", "fractional derivative", "fractional integrator", etc. In the following examples, the discrete transfer Fcn blocks are used, as only they can be properly compiled into C language using MATLAB real-time environment and implemented to the functional unit DC/AC converter.

In the studied SG model, three equations from the equation system (13) contain derivatives represented by the Laplace operator s to the power of 1/2. After some transformations of the mathematical equations to calculate certain machine values (e.g., i_{1d}, i_{1q} and φ_{2d}), one obtains the equations with the half-order derivatives and integrals. In the MATLAB/Simulink environment, they can be modelled as shown in Fig. 2–4.

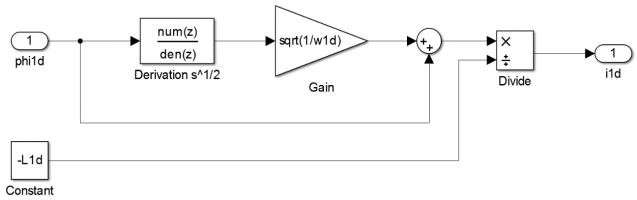

Fig. 2. Current i_{1d} calculation in MATLAB/Simulink software

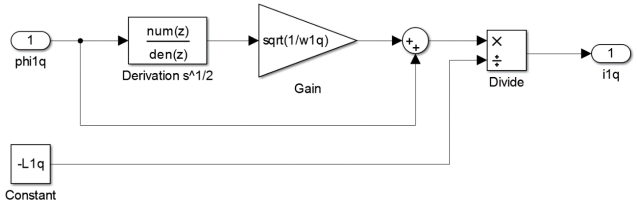

Fig. 3. Current i_{1q} calculation in MATLAB/Simulink software

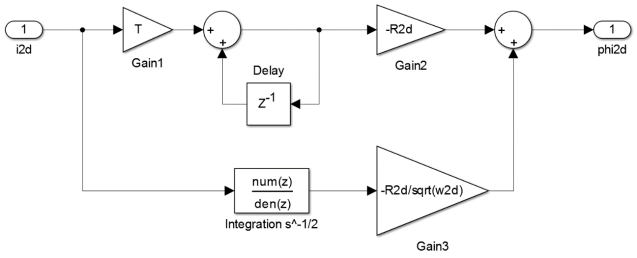

Fig. 4. Flux φ_{2d} calculation in MATLAB/Simulink software

Numerators and denominators (num(z), den(z)) of the above present derivatives and integrals were calculated in MATLAB using *ora_foc* (Oustaloup-recursive-approximation for fractional order differentiator) and *c2d* (convert model from continuous to discrete time) functions. It is worth noting that the *c2d* function, which converts any model from continuous to discrete time, works more stable if the continuous time system is introduced in the form of a state-space model instead of a transfer function.

The following figures (Fig. 5–8) present the results of the Oustaloup approximation of the discrete half-order integral and derivative in comparison to ideal first-order ones. The Oustaloup approximation order N was equal to 2 and 5 for comparison purposes. The calculation step of the simulation model was set to 1 ms.

Figure 5 and Fig. 7 indicate that the properties of the half-order integral and derivative are preserved, i.e., the magnitude asymptote changes by 10 dB per decade, while the phase asymptote is −45°. Also, the feature of including slow and fast dynamics at the same time is noticeable in Fig. 6, where the integral starts to respond very quickly, and then stabilizes to reach the final slope value. The order N of the Oustaloup approximation has no significant impact on the time response (Fig. 6 and Fig. 8) as it has in the frequency domain (Fig. 5 and Fig. 7). Nevertheless, to achieve an acceptable accuracy as well as to overcome the stability problems present for higher order approximations the order N was chosen equal to 5 [43]. Therefore, in further

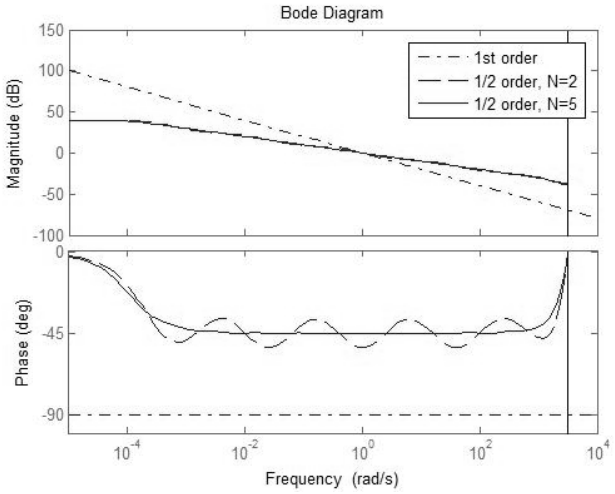

Fig. 5. Bode diagram of the discrete half-order and first-order integral

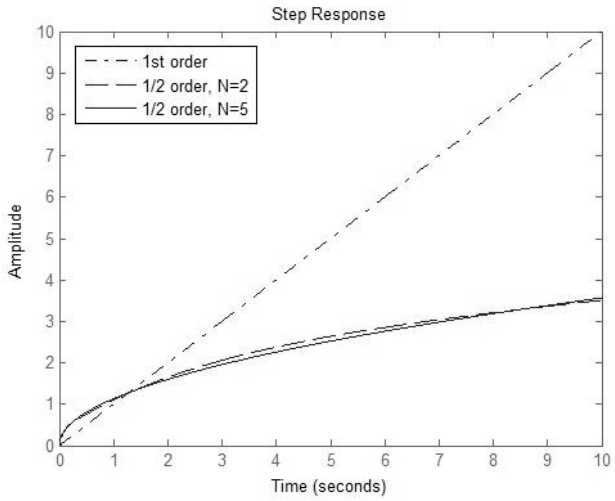

Fig. 6. Step response of the discrete half-order and first-order integral

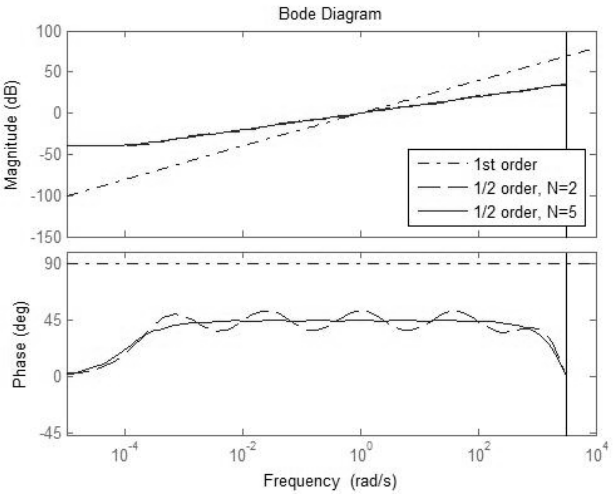

Fig. 7. Bode diagram of the discrete half-order and first-order derivative

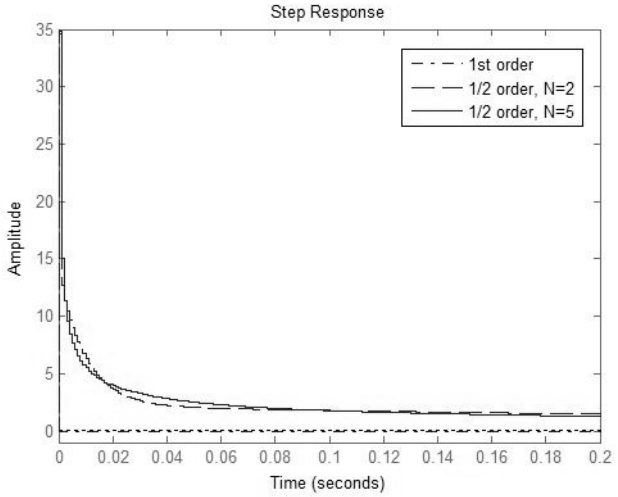

Fig. 8. Step response of the discrete half-order and first-order derivative

studies, the discrete form of the Oustaloup approximations of the half-order integrals and derivatives are used in the MATLAB/Simulink SG model.

4. PHIL CONCEPT OF AUTONOMOUS POWER SYSTEM WITH SG

The proposed PHIL system is composed of functional units, functional unit controllers, and control and communication peripherals (Fig. 9) [44].

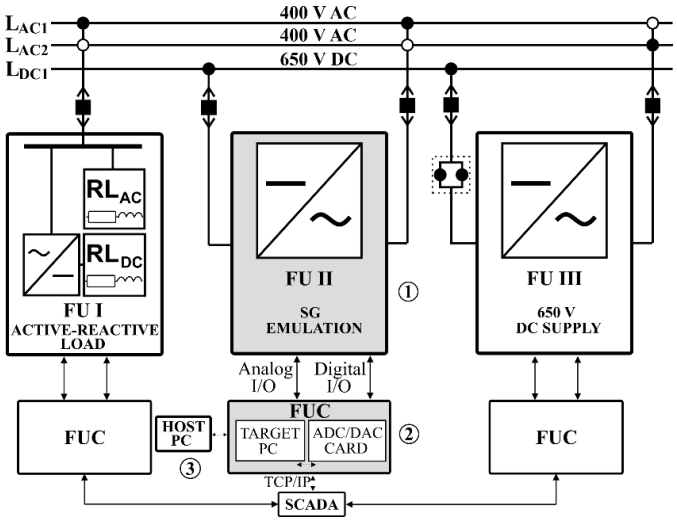

Fig. 9. PHIL system hardware diagram: functional units (1), functional unit controllers (2), control/communication peripherals (3)

The system emulates the behaviour of SG operating in an isolated power system by the controlled bidirectional DC/AC power converter (marked as 1 in Fig. 9). This energy source is subjected to sudden active-reactive load changes to imitate the real SG working conditions in an autonomous power generation systems. During transient states, the voltage and frequency variations are observed, which is the subject of further discussion.

The commercial-grade power converters are designed to reproduce the set voltage value and frequency. Therefore, the proposed discrete non-integer order Simulink model of SG was developed to calculate the reference output AC voltage amplitude (*V_AC_model*) and frequency (calculated based on *wm*) for the power converter based on the given T_l torque of the prime mover (*Tl_in*), measured load current (*I_AC*), phase voltage, and frequency for active (*P_AC*) and reactive powers (*Q_AC*) calculation. The Simulink real-time kernel can execute the real-time control algorithm every 1 ms. Figure 10 shows the MATLAB/Simulink I/O signals of the SG model for the PHIL approach implementation.

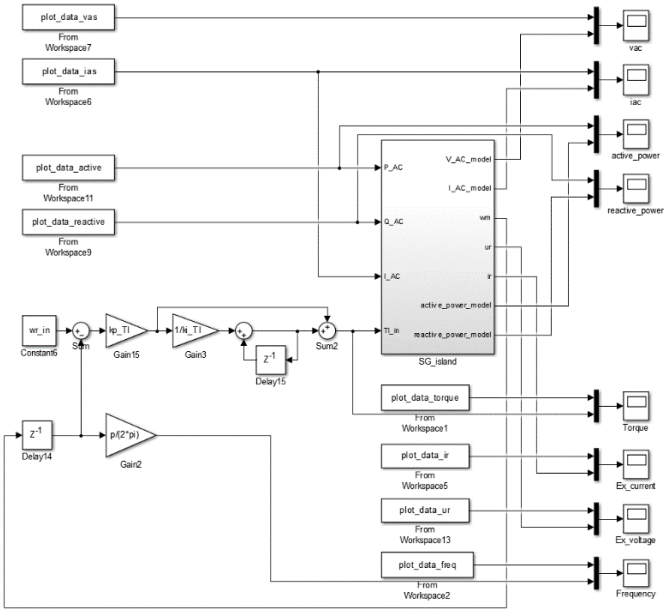

Fig. 10. MATLAB/Simulink I/O signals of the emulated SG

All of the model parameters, initial values, and input signals were initialized in m-file and loaded to the MATLAB Workspace memory. For accuracy studies, the model facilitates observation of all the internal machine variables and values, e.g., active and reactive powers, load voltage and current, excitation voltage and current, speed, etc. However, the potentially used DC/AC power converter needs only the armature voltage and frequency as the input values.

5. EXPERIMENTAL SETUP

To validate and compare the proposed non-integer order SG model, the series of tests were performed on the Elmor GCh114a/4 3-phase, 4-pole, 125 kVA (0.8 pf), 400 V, wye connected salient pole SG using controlled short-circuit measurement setup (Fig. 11). The rated data of the SG can be found in Appendix. The SG was tested on the dynamometer test stand with speed and torque control (Fig. 12). Measurements of voltages and currents during active-reactive load (40 kW and 20 kVar at 400 VAC) switch on and off were performed using LEM® current transducers and the ZES ZIMMER LMG670 power analyzer.

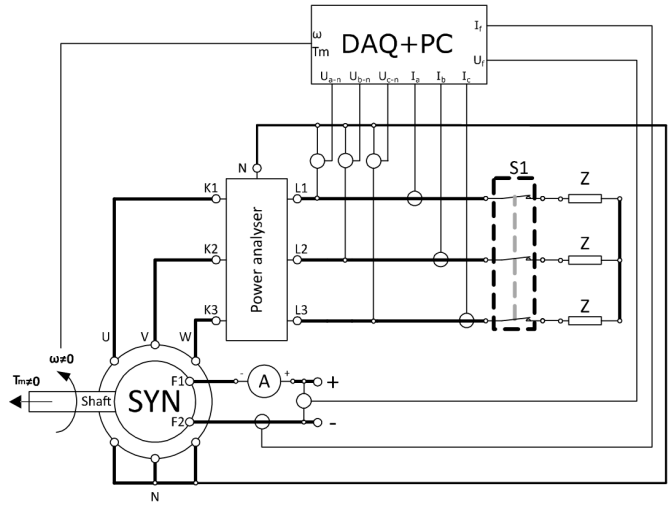

Fig. 11. Diagram of short-circuit measurement setup for SG activere-active load (Z) change tests

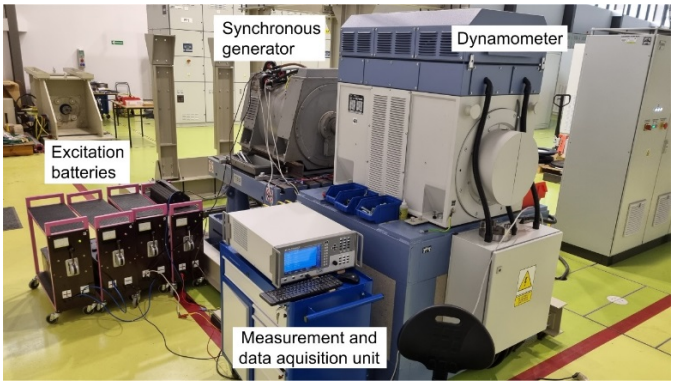

Fig. 12. Dynamometer test stand with studied SG

6. DEVELOPED MODEL VALIDATION RESULTS

To validate the developed model, the measurement results of load current, active, and reactive powers performed on the Elmor SG connected to the various active-reactive loads were given to the MATLAB/Simulink model input. The model response was then compared with corresponding measurements. The following figures (Fig. 13–16) present the comparison of the integer and non-integer order model of SG while connected to an example active-reactive load of 40 kW and 20 kVar at 400 VAC. The armature RMS voltage drop observed in Fig. 13 is due to the lack of an automatic voltage regulator (AVR).

For each simulated waveform the mean squared error (MSE) as referred to measurements was calculated.

Figure 13 shows that the non-integer order model is more accurate during the transient state than the classical one. Indeed, the discretization of the non-integer order model and Oustaloup approximation of its fractional order integrals and derivatives did not influence significantly the model response accuracy in the transient state. Whereas, the difference between simulations and measurements in steady state is due to simplifications made for both models, i.e., lack of saturation effect implementation. Actually, in industrial power generation units, the influence of

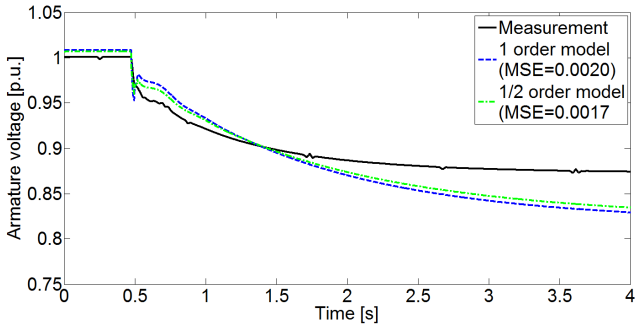

Fig. 13. Measured and simulated SG armature RMS voltage

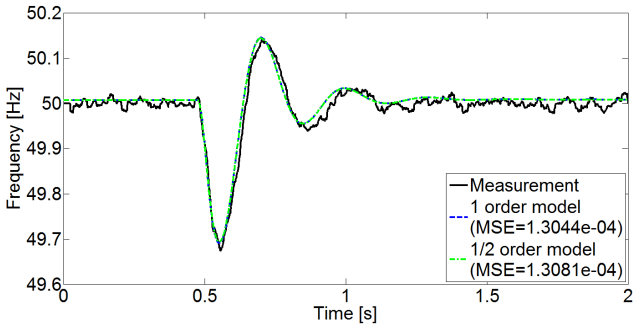

Fig. 14. Measured and simulated SG armature voltage frequency

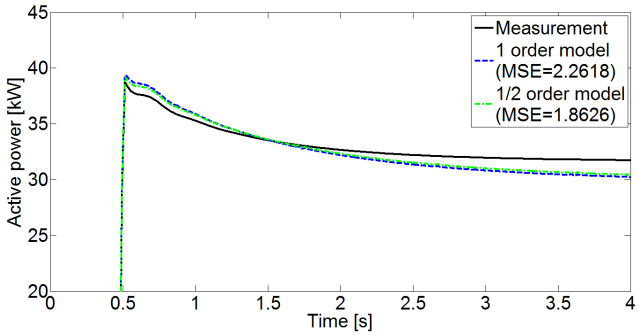

Fig. 15. Measured and simulated SG active power

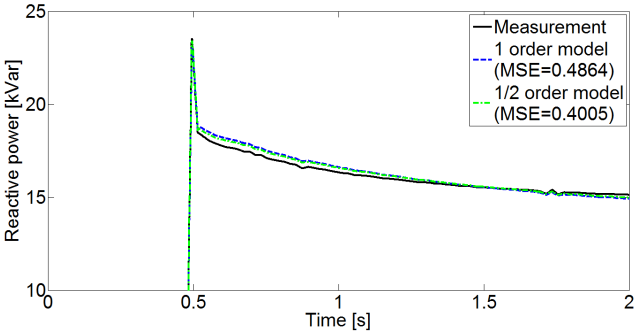

Fig. 16. Measured and simulated SG reactive power

saturation of the SG core on the output voltage amplitude is suppressed by the use of the AVR. However, voltage frequency is reproduced with high accuracy by both models. Therefore, the control signals, i.e., voltage and frequency set points for

the DC/AC power converter calculated based on the non-integer order SG model can be successfully applied in the proposed PHIL platform.

The following figures (Fig. 15 and Fig. 16) show the reproduced active and reactive powers, respectively.

One can notice that as before, the non-integer order SG model responds more accurately than the classical one, which can translate into higher precision of the designed PHIL system based on the real-time control algorithm.

7. CONCLUSIONS

The first mention of the non-integer order model of SG appeared in the early 2000s. The beginning of the 21st century was the time of rapid development of this type of modelling technique. Indeed, Prof. Shantanu Das in his book from 2011 suggested that the differintegral calculus would be the calculus of the 21st century [45]. The hardware-in-the-loop and power hardware-in-the-loop modelling techniques are the new areas, where this type of modelling has become increasingly justified.

In the presented research, the discrete non-integer order model of SG was developed and prepared in the MATLAB/Simulink software for the PHIL platform based on the bidirectional DC/AC power converter. For this purpose, the half-order derivatives and integrals from the differential equations were approximated using the Oustaloup method. Such a PHIL platform used in the SG diagnostic system can support fault-condition detection in a power generation unit performance. Finally, the model was successfully validated on the measurements carried out on the real 125 kVA SG connected to the active-reactive loads of different values and compared with the classical integer order SG model. The results of the study show greater compliance of the non-integer order model with measurements in transient states than the classical one. This proved that the use of fractional order system approximations does not deteriorate the overall accuracy of the developed model. The ability to compile such a discrete non-integer order model into the C language facilitates the successful implementation of the model on the PHIL platforms based on real-time control algorithms.

The proposed PHIL approach based on the non-integer order model has the potential for further development. To improve the performance and scope of application of the emulation platform, additional physical phenomena, e.g., saturation effect should be incorporated into the model. The model should be also run on the more powerful target PC to increase the sampling/calculation frequency. Furthermore, future studies will focus on running the developed SG model on the self-designed power converter to enable precise harmonics generation and analysis.

APPENDIX

Elmor GCh114o/4 rated data:

- Nominal frequency: $f_n = 50$ Hz.
- Nominal voltage: $U_n = 400$ V.
- Nominal power: $S_n = 125$ kVA.
- Nominal current: $I_n = 180$ A.
- Power Factor: PF = 0.8.

Identified Elmor GCh114o/4 parameters in SI units (stator side) using the SSFR test procedure:

L_{ls} = 0.4e-3 H, L_{md} = 3.8e-3 H, L_{mq} = 2.8e-3 H, L_{1d} = 0.3 H, ω_{1d} = 5.15 rad/s, L_{1q} = 0.16 H, ω_{1q} = 5.66 rad/s, R_{2d} = 12.2e-3 Ω, ω_{2d} = 1e-3 rad/s, L_{f12d} = 1e-6 H, r_{kq} = 4.1e-3 Ω, L_{lkq} = 4.3e-3 H, L_{lfd} = 0.12e-3 H, r_s = 33e-3 Ω, r_{fd} = 2.3e-3 Ω.

Base values:

- Frequency: $f_b = 50$ Hz.
- Pulsation: $\omega_b = 2\pi f_b = 314.1593$ rad/s.
- Impedance: $Z_b = Un2/S_n = 1.28$ Ω.
- Inductance: $L_b = Z_b/\omega_b = 0.0041$ H

REFERENCES

[1] E. Kuhn, C. Forgez, and G. Friedrich, "Modeling diffusive phenomena using non integer derivatives application NiMH batteries," *EPJ Appl. Phys.*, vol. 25, no. 3, pp. 183–190, Mar. 2004, doi: 10.1051/epjap:2004009.

[2] Z. Qi, D. Chen, and L. Shan, "Fractional Order Modeling of PEMFC Temperature," in *Proc. 3rd International Conference on Electric and Electronics*, 2013, pp. 257–260. doi: 10.2991/eeic-13.2013.60.

[3] K. Oprzędkiewicz, K. Dziedzic, and Ł. Więckowski, "Non integer order, discrete, state space model of heat transfer process using Grünwald-Letnikov operator," *Bull. Pol. Acad. Sci. Tech. Sci.*, vol. 67, no. 5, pp. 905–914, Nov. 2019, doi: 10.24425/bpasts.2019.130873.

[4] S. Irshad, S. Jahan, A.Z. Jan, K. Kędzia, A.H. Majeed, and F. Khan, "Fractional order transient free-convection flow in a channel: application of the optimal homotopy asymptotic method," *Arch. Thermodyn.*, vol. 45, no. 2, pp. 139–144, May 2024, doi: 10.24425/ather.2024.150860.

[5] M.U. Iftikhar, D. Riu, F. Druart, S. Rosini, Y. Bultel, and N. Retičre, "Dynamic modeling of proton exchange membrane fuel cell using non-integer derivatives," *J. Power Sources*, vol. 160, no. 2 spec. iss., pp. 1170–1182, Oct. 2006, doi: 10.1016/j.jpowsour.2006.03.044.

[6] V. Martynyuk and M. Ortigueira, "Fractional model of an electrochemical capacitor," *Signal Proces.*, vol. 107, pp. 355–360, 2015, doi: 10.1016/j.sigpro.2014.02.021.

[7] A. Jalloul, J.C. Trigeassou, K. Jelassi, and P. Melchior, "Fractional order modeling of rotor skin effect in induction machines," *Nonlinear Dyn.*, vol. 73, no. 1–2, pp. 801–813, Jul. 2013, doi: 10.1007/s11071-013-0833-8.

[8] D.M. Riu, N.M. Retičre, and M.S. Ivančs, "Induced currents modeling by half-order systems application to hydro- and turbo-alternators," *IEEE Trans. Energy Convers.*, vol. 18, no. 1, pp. 94–99, Mar. 2003, doi: 10.1109/TEC.2002.808385.

[9] D. Ziani, S.-E. Bendimerad, and A. Ayad, "Influence of the variety of steel tube materials on the impedance behavior of non-destructive Eddy current testing," *Diagnostyka*, vol. 24, no. 2, pp. 1–6, May 2023, doi: 10.29354/diag/163092.

[10] A. Oustaloup and X. Moreau, "Mechanical Version of the CRONE Suspension," in *Lecture Notes in Control and Information Sciences*, vol. 407, Springer Verlag, 2010, pp. 99–112. doi: 10.1007/978-3-642-16135-3_9.

[11] D. Riu, M. Montaru, and Y. Bultel, "Time domain simulation of Li-ion batteries using non-integer order equivalent electrical

circuit," *Commun. Nonlinear Sci. Numer. Simul.*, vol. 18, no. 6, pp. 1454–1462, Jun. 2013, doi: 10.1016/j.cnsns.2012.06.028.

[12] M. Lewandowski and M. Orzyłowski, "Fractional-order models: The case study of the supercapacitor capacitance measurement," *Bull. Pol. Acad. Sci. Tech. Sci.*, vol. 65, no. 4, pp. 449–457, Aug. 2017, doi: 10.1515/bpasts-2017-0050.

[13] P. Skruch and W. Mitkowski, "Fractional-order models of the ultracapacitors," in *Lecture Notes in Electrical Engineering*, 2013, pp. 281–293. doi: 10.1007/978-3-319-00933-9-26.

[14] M.A. Taleb, E. Godoy, O. Bethoux, and D. Irofti, "PEM fuel cell fractional order modeling and identification," *IFAC Proc. Vol.*, vol. 47, no. 3, pp. 2125–2131, 2014, doi: 10.3182/20140824-6-ZA-1003.01627.

[15] D. Ivanov, "Identification of Fractional Models of an Induction Motor with Errors in Variables," *Fractal Fract.*, vol. 7, no. 6, p. 485, Jun. 2023, doi: 10.3390/fractalfract7060485.

[16] J. Staszak, "Solid-Rotor Induction Motor Modeling Based on Circuit Model Utilizing Fractional-Order Derivatives," *Energies*, vol. 15, no. 17, p. 6371, Aug. 2022, doi: 10.3390/en15176371.

[17] A.K. Kamath *et al.*, "Modeling of transformer characteristics using fractional order transfer functions," in *2009 IEEE International Conference on Control and Automation, ICCA 2009*, 2009, pp. 2123–2128. doi: 10.1109/ICCA.2009.5410191.

[18] B. Yildirim, M. Gheisarnejad, and M.H. Khooban, "A Robust Non-Integer Controller Design for Load Frequency Control in Modern Marine Power Grids," *IEEE Trans. Emerg. Top. Comput. Intell.*, vol. 6, no. 4, pp. 852–866, Aug. 2022, doi: 10.1109/TETCI.2021.3114735.

[19] S. Racewicz, F. Kutt, M. Michna, and Ł. Sienkiewicz, "Comparative Study of Integer and Non-Integer Order Models of Synchronous Generator," *Energies*, vol. 13, no. 17, p. 4416, Aug. 2020, doi: 10.3390/en13174416.

[20] A. Oustaloup, O. Cois, P. Lanusse, P. Melchior, X. Moreau, and J. Sabatier, "The crone aproach: Theoretical developments and major applications," in *IFAC Proc. Vol. (IFAC-PapersOnline)*, 2006, pp. 324–354. doi: 10.3182/20060719-3-pt-4902.00059.

[21] S. Abrazeh *et al.*, "Virtual Hardware-in-the-Loop FMU Co-Simulation Based Digital Twins for Heating, Ventilation, and Air-Conditioning (HVAC) Systems," *IEEE Trans. Emerg. Top. Comput. Intell.*, vol. 7, no. 1, pp. 65–75, Feb. 2023, doi: 10.1109/TETCI.2022.3168507.

[22] N. Sharma, G. Mademlis, Y. Liu, and J. Tang, "Evaluation of Operating Range of a Machine Emulator for a Back-to-Back Power-Hardware-in-the-Loop Test Bench," *IEEE Trans. Ind. Electron.*, vol. 69, no. 10, pp. 9783–9792, Oct. 2022, doi: 10.1109/TIE.2022.3142421.

[23] J. Noon *et al.*, "A Power Hardware-in-the-Loop Testbench for Aerospace Applications," in *2020 IEEE Applied Power Electronics Conference and Exposition (APEC)*, IEEE, Mar. 2020, pp. 2884–2891. doi: 10.1109/APEC39645.2020.9124299.

[24] W. Chen *et al.*, "DC-Distributed Power System Modeling and Hardware-in-the-Loop (HIL) Evaluation of Fuel Cell-Powered Marine Vessel," *IEEE J. Emerg. Sel. Top. Ind. Electron.*, vol. 3, no. 3, pp. 797–808, Jul. 2022, doi: 10.1109/JESTIE.2021.3139471.

[25] W. Chen, T. Liang, and V. Dinavahi, "Comprehensive Real-Time Hardware-In-the-Loop Transient Emulation of MVDC Power Distribution System on Nuclear Submarine," *IEEE Open J. Ind. Electron. Soc.*, vol. 1, pp. 326–339, 2020, doi: 10.1109/OJIES.2020.3036731.

[26] K.-W. Heo, H.-J. Choi, and J.-H. Jung, "Real-time test-bed system development using power hardware-in-the-loop (PHIL) simulation technique for reliability test of DC nano grid," *J. Power Electron.*, vol. 20, no. 3, pp. 784–793, May 2020, doi: 10.1007/s43236-020-00075-x.

[27] L.G. Zadeh, T.K.A. Brekken, A. Fern, and A.H. Shahbaz, "Hardware in the Loop Wave Energy Converter Control under Control Faults and Model Mismatch," *IEEE Trans. Sustain. Energy*, pp. 1–10, 2023, doi: 10.1109/TSTE.2023.3272537.

[28] Q. Zhao, K. Liao, J. Yang, Z. He, and Y. Xu, "Aging Rate Equalization Strategy for Battery Energy Storage Systems in Microgrids," *IEEE Trans. Smart Grid*, vol. 15, no. 1, pp. 136–148, Jan. 2024, doi: 10.1109/TSG.2023.3280226.

[29] Y. Liu, L. Ralikalakala, P. Barendse, and P. Pillay, "Power Electronic Converter Based Induction Motor Emulator With Stator Winding Faults," *IEEE Trans. Ind. Electron.*, vol. 70, no. 5, pp. 4440–4449, May 2023, doi: 10.1109/TIE.2022.3189099.

[30] G. Abdelhak, B. Sid Ahmed, and R. Djekidel, "Fault diagnosis of induction motors rotor using current signature with different signal processing techniques," *Diagnostyka*, vol. 23, no. 2, pp. 1–9, Mar. 2022, doi: 10.29354/diag/147462.

[31] M. Basaran and M. Fidan, "Induction motor fault classification via entropy and column correlation features of 2D represented vibration data," *Eksploat. i Niezawodn. – Maint. Reliab.*, vol. 23, no. 1, pp. 132–142, Mar. 2021, doi: 10.17531/ein.2021.1.14.

[32] Ł. Breńkacz, P. Bagiński, M. Adamowicz, and S. Giziewski, "Failure analysis of a high-speed induction machine driven by a SiC-inverter and operating on a common shaft with a high-speed generator," *Eksploat. i Niezawodn. – Maint. Reliab.*, vol. 24, no. 1, pp. 177–185, Mar. 2022, doi: 10.17531/ein.2022.1.20.

[33] G. Lauss *et al.*, "A Framework for Sensitivity Analysis of Real-Time Power Hardware-in-the-Loop (PHIL) Systems," *IEEE Access*, vol. 10, pp. 101305–101318, 2022, doi: 10.1109/ACCESS.2022.3206780.

[34] S.S. Madani and A. Karimi, "Stabilization and Performance Improvement of Power-Hardware-in-the-Loop Test Using a Robust Data-Driven Method," *IEEE Trans. Instrum. Meas.*, vol. 71, pp. 1–11, 2022, doi: 10.1109/TIM.2022.3150593.

[35] F. Ashrafidehkordi, D. Kottonau, and G. De Carne, "Multi-Rate Discrete Domain Modeling of Power Hardware-in-The-Loop Setups," *IEEE Open J. Power Electron.*, vol. 4, pp. 539–548, 2023, doi: 10.1109/OJPEL.2023.3283035.

[36] S. Racewicz, D.M. Riu, N.M. Retiere, and P.J. Chrzan, "Half-Order Modeling of Saturated Synchronous Machine," *IEEE Trans. Ind. Electron.*, vol. 61, no. 10, pp. 5241–5248, Oct. 2014, doi: 10.1109/TIE.2014.2301741.

[37] S. Racewicz, D. Riu, N. Retiere, and P. Chzran, "Non linear half-order modeling of synchronous machine," in *2009 IEEE International Electric Machines and Drives Conference*, IEEE, May 2009, pp. 778–783. doi: 10.1109/IEMDC.2009.5075292.

[38] S. Racewicz, P.J. Chrzan, D.M. Riu, and N.M. Retiere, "Time domain simulations of synchronous generator modelled by half-order system," in *IECON Proceedings (Industrial Electronics Conference)*, 2012, pp. 2074–2079. doi: 10.1109/IECON.2012.6388739.

[39] IEEEStd115, "IEEE Guide: Test Procedures for Synchronous Machines Part I – Acceptance and Performance Testing Part II – Test Procedures and Parameter Determination for Dynamic Anal-

ysis," *IEEE Std 115*, pp. 1–219, 2010, doi: 10.1109/IEEESTD.2010.5464495.

[40] A. Oustaloup, O. Cois, and L. Le Lay, *Représentation et identification par modčle non entier*. Hermes Science Publications, 2005. Accessed: Nov. 14, 2019. [Online]. Available: https://www.lavoisier.fr/livre/electricite-electronique/representation-et-identification-par-modele-non-entier/oustaloup/descriptif-9782746210868

[41] A. Oustaloup, F. Levron, B. Mathieu, and F.M. Nanot, "Frequency-band complex noninteger differentiator: characterization and synthesis," *IEEE Trans. Circuits Syst. I Fundam. Theory Appl.*, vol. 47, no. 1, pp. 25–39, 2000, doi: 10.1109/81.817385.

[42] Z. Li, L. Liu, S. Dehghan, Y. Chen, and D. Xue, "A review and evaluation of numerical tools for fractional calculus and fractional order controls," *Int. J. Control*, vol. 90, no. 6, pp. 1165–1181, Jun. 2017, doi: 10.1080/00207179.2015.1124290.

[43] J. Baranowski, W. Bauer, M. Zagorowska, T. Dziwinski, and P. Piatek, "Time-domain Oustaloup approximation," in *2015 20th International Conference on Methods and Models in Automation and Robotics (MMAR)*, IEEE, Aug. 2015, pp. 116–120. doi: 10.1109/MMAR.2015.7283857.

[44] S. Racewicz, F. Kutt, and Ł. Sienkiewicz, "Power Hardware-In-the-Loop Approach for Autonomous Power Generation System Analysis," *Energies*, vol. 15, no. 5, p. 1720, Feb. 2022, doi: 10.3390/en15051720.

[45] S. Das, *Functional Fractional Calculus*. Berlin, Heidelberg: Springer Berlin Heidelberg, 2011. doi: 10.1007/978-3-642-20545-3.